









Heart–gut microbiota communication determines the severity of cardiac injury after myocardial ischaemia/reperfusion

Jinxuan Zhao ^{1†}, Qi Zhang^{1†}, Wei Cheng^{2†}, Qing Dai¹, Zhonghai Wei¹, Meng Guo¹, Fu Chen ¹, Shuaihua Qiao ¹, Jiaxin Hu ¹, Junzhuo Wang¹, Haiting Chen¹, Xue Bao ¹, Dan Mu³, Xuan Sun ¹, Biao Xu ^{1*}, and Jun Xie ^{1*}

¹Department of Cardiology, MOE Key Laboratory of Model Animal for Disease Study, Nanjing Drum Tower Hospital, The Affiliated Hospital of Nanjing University Medical School, Nanjing University, No. 321 Zhongshan Road, Nanjing 210008, China; ²Department of General Surgery, Jiangsu Province Hospital of Chinese Medicine, Affiliated Hospital of Nanjing University of Chinese Medicine, No. 155 Hanzhong Road, Nanjing 210000, China; and ³Department of Radiology, Nanjing Drum Tower Hospital, The Affiliated Hospital of Nanjing University Medical School, Nanjing University, No. 321 Zhongshan Road, Nanjing 210008, China

Received 31 March 2022; revised 25 October 2022; accepted 11 November 2022; online publish-ahead-of-print 30 January 2023

Aims

Recent studies have suggested a key role of intestinal microbiota in pathological progress of multiple organs via immune modulation. However, the interactions between heart and gut microbiota remain to be fully elucidated. The aim of the study is to investigate the role of gut microbiota in the post-ischaemia/reperfusion (I/R) inflammatory microenvironment.

Methods and results

Here, we conducted a case-control study to explore the association of gut bacteria translocation products with inflammation biomarkers and I/R injury severity in ST-elevation myocardial infarction patients. Then, we used a mouse model to determine the effects of myocardial I/R injury on gut microbiota dysbiosis and translocation. Blooming of Proteobacteria was identified as a hallmark of post-I/R dysbiosis, which was associated with gut bacteria translocation. Abrogation of gut bacteria translocation by antibiotic cocktail alleviated myocardial I/R injury via mitigating excessive inflammation and attenuating myeloid cells mobilization, indicating the bidirectional heart–gut–microbiome–immune axis in myocardial I/R injury. Glucagon-like peptide 2 (GLP-2), an endocrine peptide produced by intestinal L-cells, was used in the experimental myocardial I/R model. GLP-2 administration restored gut microbiota disorder and prevented bacteria translocation, eventually attenuated myocardial I/R injury through alleviating systemic inflammation.

Conclusion

Our work identifies a bidirectional communication along the heart–gut–microbiome–immune axis in myocardial I/R injury and demonstrates gut bacteria translocation as a key regulator in amplifying inflammatory injury. Furthermore, our study sheds new light on the application of GLP-2 as a promising therapy targeting gut bacteria translocation in myocardial I/R injury.

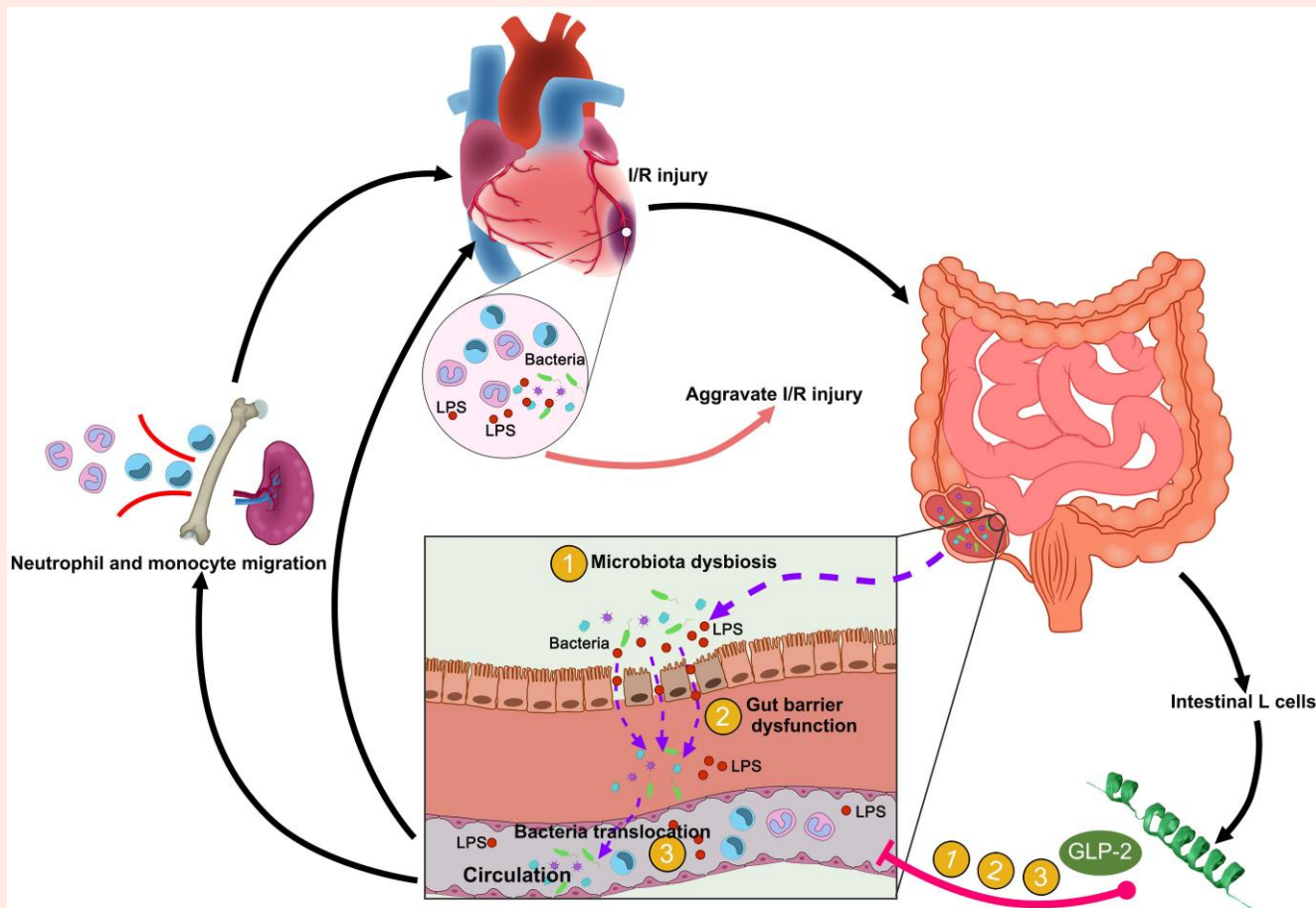
* Corresponding author. Tel/fax: 86 25 68182812, E-mail: xiejun@nju.edu.cn (J.X.); Tel/fax: 86 25 83106666, E-mail: xubiao62@nju.edu.cn (B.X.)

† Jinxuan Zhao, Qi Zhang, and Wei Cheng contributed equally to this article.

© The Author(s) 2023. Published by Oxford University Press on behalf of the European Society of Cardiology.

This is an Open Access article distributed under the terms of the Creative Commons Attribution-NonCommercial License (<https://creativecommons.org/licenses/by-nc/4.0/>), which permits non-commercial re-use, distribution, and reproduction in any medium, provided the original work is properly cited. For commercial re-use, please contact journals.permissions@oup.com

Graphical Abstract



Schematic diagram showing the role of the heart–gut–microbiome–immune axis in myocardial I/R injury. Application of glucagon-like peptide 2 targeting heart–intestine axis might be a potential strategy to alleviate I/R injury.

Keywords

Myocardial ischaemia/reperfusion injury • Inflammation • Gut microbiota dysbiosis • Bacteria translocation • Glucagon-like peptide 2

1. Introduction

Acute myocardial infarction (AMI) is one of the leading causes of morbidity and mortality worldwide. Nowadays, primary percutaneous coronary intervention is widely used to restore blood flow, thereby reducing the infarct size. However, the process of reperfusion itself may induce further cardiac deterioration, known as myocardial ischaemia/reperfusion (I/R) injury.¹ Microvascular obstruction (MVO) represents a pivotal manifestation of myocardial I/R injury and has been identified as an independent risk factor for poor prognosis in patients with AMI.² Accumulating evidence indicated that the inflammatory cascade triggered by I/R injury is considered one of the main mechanisms of MVO formation.³ Following myocardial I/R, a variety of damage-associated molecules are released from necrotic cardiac resident cells, thus inducing an inflammatory cascade within the heart. Though inflammation is essential for converting necrotic tissue into scar, prolonged or excessive inflammation may lead to sustained tissue damage and improper healing. However, the intricate mechanisms underlying the occurrence of excessive inflammation following myocardial I/R injury are not fully elucidated.

Intestinal commensal microbes, the most abundant symbiotic organisms in the body, have emerged as a potent regulator of the host immune

system. Emerging evidence suggests that an imbalance of gut microbiota communities has been associated not only with intestinal pathological conditions but also with many extra-intestinal diseases, such as obesity,⁴ cancer,⁵ diabetes,⁶ and cardiovascular diseases.^{7,8} Recent studies shed light on the crosstalk between intestinal microbiota and severity of myocardial infarction (MI).^{9,10} A current report by Tang *et al.*¹¹ has demonstrated that depletion of intestinal microbiota influences post-MI cardiac inflammation and outcome in an experimental MI model. Additionally, circulating levels of lipopolysaccharides (LPS) and bacterial ribosomal DNA (rDNA) are significantly increased in ST-elevation myocardial infarction (STEMI) patients and are associated with poor prognosis.^{12–14} These results provide the first hints suggesting the role of bacterial invasion and translocation in the development of MI. However, the impact of myocardial I/R injury on gut microbiota homeostasis and the contribution of I/R-induced microbiota alterations on peripheral immune activation as well as inflammatory response in myocardium remain largely unknown. Therefore, the objective of this study is to explore gut microbiota alterations under myocardial I/R injury and their role in the post-I/R inflammatory microenvironment.

Our study unravels the role of the heart–gut–microbiome–immune axis in myocardial I/R injury and provides novel therapeutic insight into

gut-targeted therapeutic strategies to improve the prognosis of AMI in the future.

2. Methods

The human study was performed in accordance with the Declaration of Helsinki and was approved by the Institutional Ethics Committee of Nanjing Drum Tower Hospital (Approval No. 2019-190-01). Informed consent was obtained from each study participant. All procedures with animals were approved by the Institutional Ethics Committee of Nanjing Drum Tower Hospital (Approval No. 20011141) and performed in accordance with the guidelines from Directive 2010/63/EU of the European Parliament. After the study, all animals were anaesthetized by isoflurane inhalation (1.5–2%) and then euthanized by cervical dislocation. Detailed descriptions are provided in the [Supplementary Material](#).

2.1 Statistical analysis

Continuous variables with normal distribution were expressed as mean \pm standard deviation. Categorical variables were reported as counts (percentage). Differences between percentages were assessed by χ^2 test or Fisher's exact test. The groups containing normally distributed parametric data were tested using a two-way Student's *t*-test (for two groups) or one-way analysis of variance (ANOVA) followed by Tukey's multiple comparison test (for more than two groups). Non-parametric data were compared by Mann–Whitney's *U* test. Two-way ANOVA followed by Bonferroni's multiple comparison test was used to determine differences between groups at multiple time points. Binary logistic regression was used to assess the association between clinical covariates and MVO formation (results presented as odds ratio and 95% confidence interval). Variables with $P < 0.10$ at univariable analysis were then included as covariates in multivariable analysis. Correlations between continuous variables were determined using Pearson's correlation or Spearman's correlation. The Kaplan–Meier method and Log-rank (MantelCox) test were used to construct and compare the survival curves of animals, respectively. All analyses were performed using Prism 6 software (GraphPad) and SPSS (version 18.0). Only differences with a *P*-value of less than 0.05 were considered statistically significant.

3. Results

3.1 Gut bacterial translocation was associated with inflammation and severity of I/R injury in STEMI patients

We recruited 23 healthy controls and 97 STEMI patients to explore the occurrence of intestinal microbiota translocation and its correlation with the clinical characteristics of STEMI patients. Zonulin and LPS were recognized as products and systemic markers for increased gut permeability and bacterial translocation.¹³ We found elevated levels of zonulin and LPS in the serum of STEMI patients when compared with control (*Figure 1A and B*). Same higher levels were observed in blood bacterial 16S rDNA measured by quantitative polymerase chain reaction (qPCR) (*Figure 1C*), suggesting more abundant bacteria rDNA in the systemic circulation of STEMI patients. Significant positive correlations were found between LPS, zonulin, and blood bacterial load in STEMI patients (*Figure 1D and E*), raising the possibility that intestinal bacteria might invade into blood post-MI as a consequence of enhanced gut permeability. Furthermore, we found that increased serum LPS positively correlated with infarct size and MVO size, and negatively correlated with left ventricular ejection fraction (LVEF%) in STEMI patients (*Figure 1F–H*). Meanwhile, the neutrophil–lymphocyte ratio (NLR), white blood cells, and neutrophil counts were strongly correlated with serum LPS concentration (see [Supplementary material online, Figure S1A–C](#)). However, the correlation between C-reactive protein and LPS was not significant (see [Supplementary material online, Figure S1D](#)). These findings suggested that translocation

of bacterial LPS from gut to systemic circulation might be considered a novel factor accounting for excessive activation of inflammation and severe I/R injury in STEMI patients.

Given that MVO was identified as an independent risk factor for prognosis in AMI patients and correlated with the extent of inflammation, we then explored the relationship between bacteria translocation and MVO formation. Clinical, demographic, and laboratory characteristics for STEMI patients with or without MVO were summarized in [Supplementary material online, Table S1](#). Among all the collected clinical data, C-reactive protein, peak Troponin T was significant in the univariate logistic regression analysis, but was not significant in the multivariate logistic regression analysis. Intriguingly, LPS, blood bacterial enrichment, and NLR remained significant in both the univariate and multivariate logistic regression analyses (*Figure 1I and J*; [Supplementary material online, Table S2](#)), indicating that intestinal bacterial translocation is an independent risk factor for STEMI patients with MVO.

3.2 Myocardial I/R injury-induced intestinal microbiota dysbiosis and intestinal mucosal injury

To determine the impact of myocardial I/R injury on gut microbiota, we subjected mice to 60 min of ischaemia followed by reperfusion or a sham operation and performed 16S ribosomal RNA (rRNA) gene sequencing on colonic contents of mice 3 days following the operation. According to our results, the gut microbial community structure of the myocardial I/R group was clearly distinguished from the sham group according to principal coordinate analysis (PCoA) and Anosim analysis (*Figure 2A–C*). At the phylum level, myocardial I/R injured mice displayed perturbed microbiota signatures characterized as a significant higher level of Proteobacteria compared with sham mice (*Figure 2D and F*). The main classes within Proteobacteria phylum, such as Alphaproteobacteria, Betaproteobacteria, Deltaproteobacteria, and Gammaproteobacteria, were dramatically increased in the myocardial I/R group relative to the sham group (*Figure 2E and G*). Pathogenic bacteria Gammaproteobacteria contributed mostly to the prevalence of Proteobacteria in the myocardial I/R group compared with the sham group (*Figure 2H*). At the family and genus level, hallmarks of post-myocardial I/R dysbiosis included an increase of *Escherichia*, which belong to the Enterobacteriaceae family, and a decrease of well-recognized probiotics *Lactobacillus* ([Supplementary material online, Figure S2](#)).

Since the integrity of the gut barrier was closely associated with the alteration of gut microbiota,¹⁵ we further evaluated the changes in the gut barrier after myocardial I/R injury. Morphology and histological staining of the whole intestine tract revealed significant deterioration of the intestinal mechanical barrier manifested as a higher Chiu pathological score in myocardial I/R injured mice when compared with sham mice (*Figure 2I–K*). In line with these changes, mucosal microvillus disarrangement and intestinal epithelium structure disruption were detected by transmission electron microscopy following myocardial I/R injury (*Figure 2L*). The reduced expression of tight-junction claudin-1 and occludin, critical components in the intestinal epithelial barrier, further supported the above observation (*Figure 2M and N*; [Supplementary material online, Figure S3](#)). Collectively, these results suggested that myocardial I/R injury induced obvious intestinal mucosal injury and gut barrier impairment accompanied by the disturbance of gut microbiota.

3.3 Changes in gut microbiota and intestinal mucosal injury upon myocardial I/R injury led to gut bacteria translocation

Considering gut microbiota dysbiosis and intestinal mucosal injury were observed in myocardial I/R injured mice, we sought to investigate their impact on gut leakage. Fluorescein isothiocyanate (FITC)-dextran tracing experiment showed that intestinal permeability remarkably increased after myocardial I/R injury suggesting the possibility of microbiota invasion (*Figure 3A*). We then performed 16S rRNA gene sequencing on blood

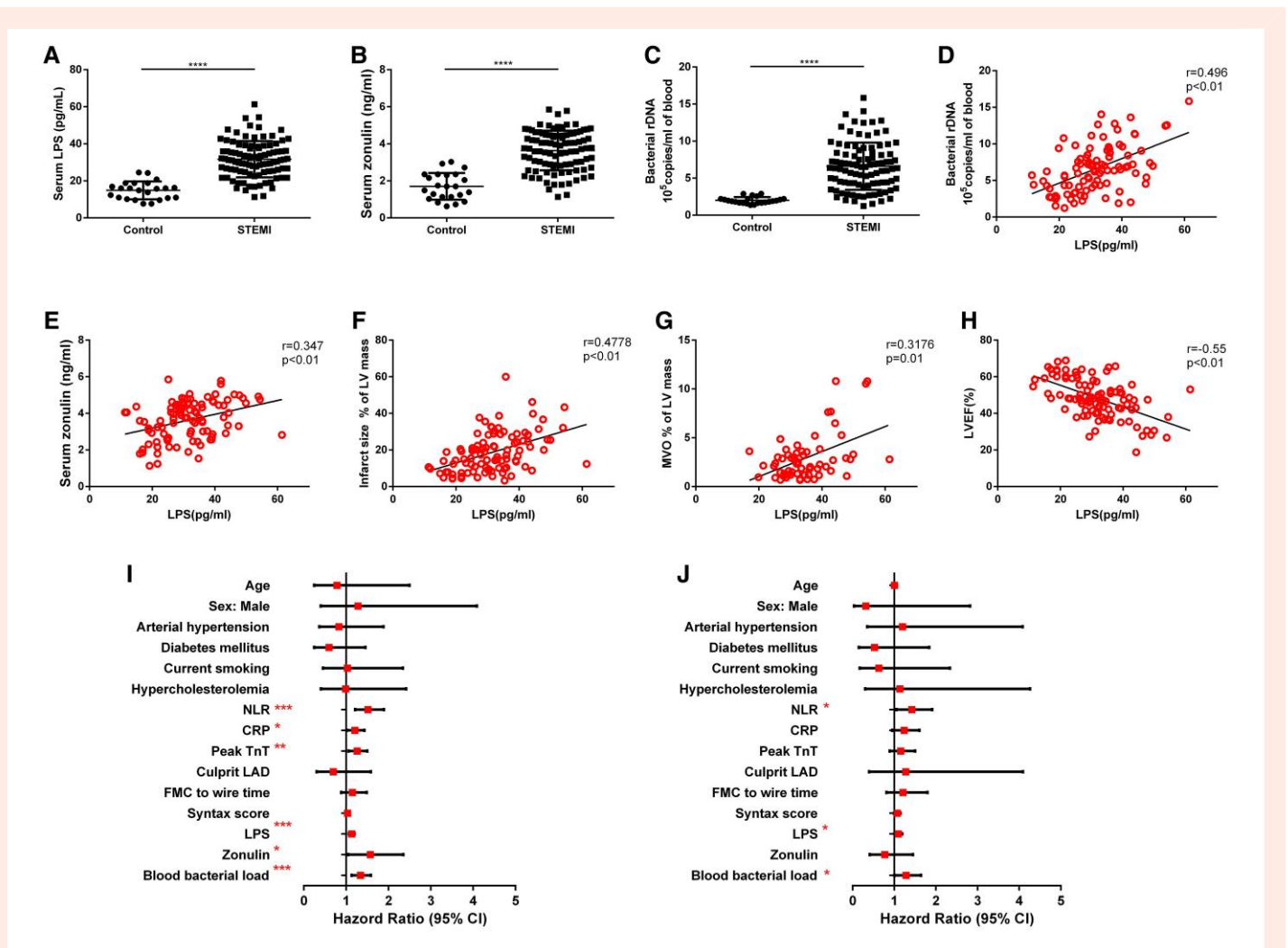


Figure 1 Increased levels of gut bacterial translocation products are associated with MVO and LV function in patients with STEMI. (A) Serum LPS, (B) serum zonulin, and (C) blood bacterial DNA load in control subjects ($n = 23$) and STEMI patients ($n = 97$). Correlation between serum LPS and blood bacterial DNA load (D), zonulin (E) in the peripheral blood of patients with STEMI ($n = 97$). (F) Correlation between serum LPS and infarct size in patients with STEMI ($n = 97$). (G) Correlation between serum LPS and MVO size in STEMI patients with MVO ($n = 60$). (H) Correlation between serum LPS and left ventricular ejection fraction (LVEF%) in patients with STEMI ($n = 97$). (I) Univariate logistic regression analysis of the risk factors for the presence of MVO in STEMI patients. (J) Multivariate logistic regression of the risk factors for the presence of MVO in STEMI patients. Values are mean \pm standard deviation (SD). Statistical significance was determined using Student's t -test for the two group comparison and the Spearman test or Pearson test for correlation analysis. * $P < 0.05$, ** $P < 0.01$, *** $P < 0.001$, **** $P < 0.0001$.

microbial profiles of sham and myocardial I/R injured mice and observed reduced species diversity following myocardial I/R injury (Figure 3B and C). The blood microbial structures of the myocardial I/R group were clearly separated from the sham group characterized as a remarkable increase of Proteobacteria and its subordinate Gammaproteobacteria class, which was similar to the changes in the intestinal microbiome to some extent (Figure 3D–F). These data further supported the hypothesis that the blood microbiota derived at least partially from the gut microbiome as a result of bacterial translocation following myocardial I/R injury. We further examined the level of bacterial-produced LPS in mouse serum and found that the LPS level increased since Day 1 post-I/R and reached the peak on Day 3. The continuous elevation of LPS in the early stage of myocardial I/R injury suggested that the translocation of bacterial LPS from gut to circulation was not a short-term effect but lasted throughout the acute phase of myocardial I/R injury (Figure 3G).

To validate the existence of gut bacterial translocation under myocardial I/R injury and determine the destination of translocated bacteria, a murine intestinal pathogen that shared a core set of virulence factors with the related human pathogens (e.g. enteropathogenic *Escherichia coli*), bioluminescent *Citrobacter rodentium*, was used in our experiments,¹⁶ which could monitor bacterial translocation accurately. As shown in Figure 3H and I, after myocardial I/R injury, bioluminescent *Citrobacter* translocated from gut into circulation, mesenteric lymph nodes (MLNs) and the extra-intestinal organs, namely spleen and heart. We also performed qPCR with specific primers for 16S rDNA and confirmed significantly higher levels of bacterial load in blood, spleen, and heart samples of myocardial I/R injured mice (Figure 3J–L). Our results first declared the presence of intestine-derived live bacteria not only in circulation but also in heart and spleen tissue following myocardial I/R injury. To characterize and visualize intra-myocardium bacteria, we applied a combination of fluorescence

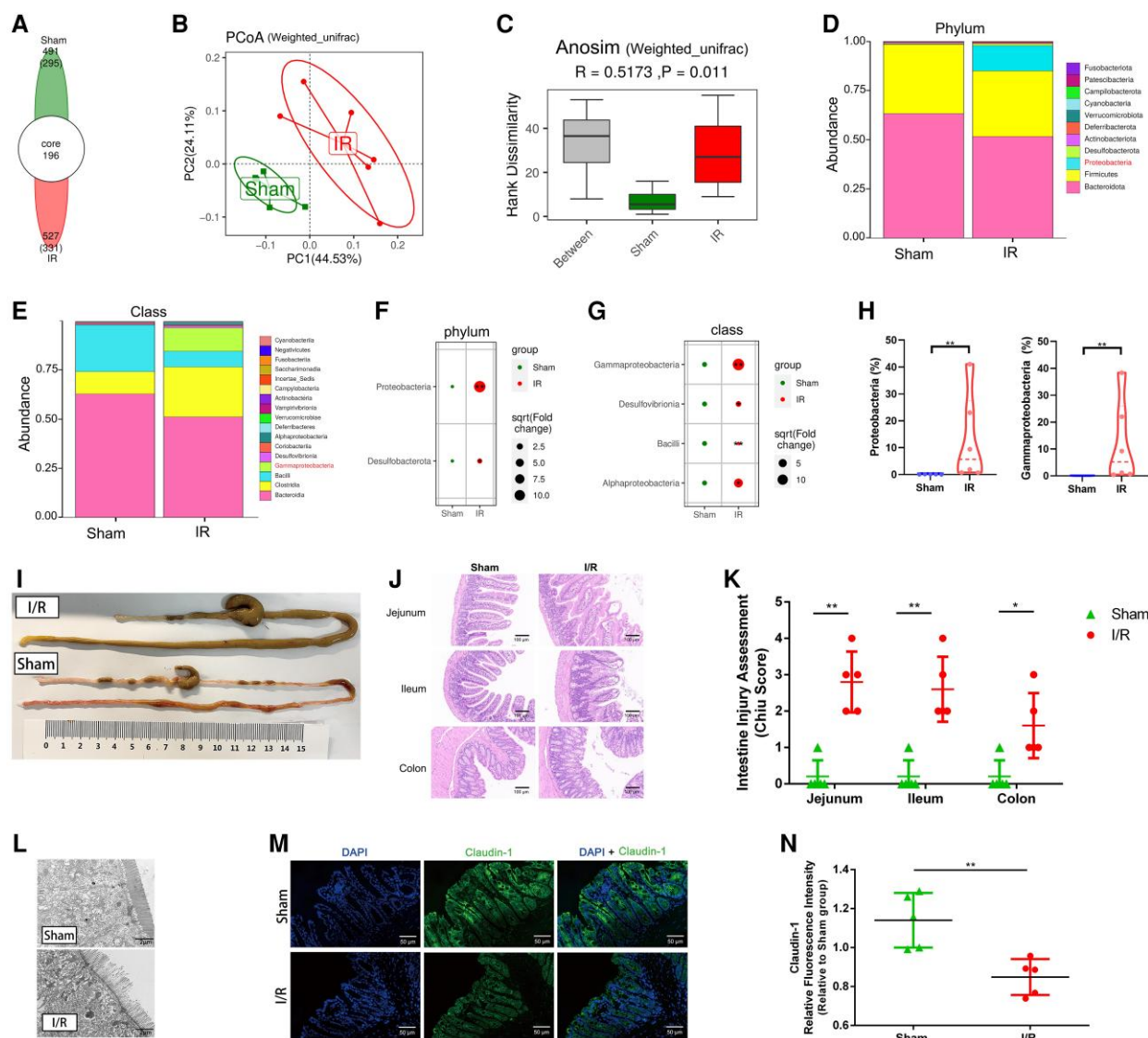


Figure 2 Myocardial I/R injured mice exhibit rapid gut microbiota dysbiosis and intestinal mucosal injury. (A) The number of common and unique Amplicon Sequence Variants (ASVs) in colon contents of sham ($n = 5$) and I/R mice ($n = 6$) 3 days after the operation. (B) PCoA of the intestinal microbiome based on weighted UniFrac distance separate the I/R group ($n = 6$) from the sham group ($n = 5$). (C) Anosim similarity analysis based on weighted UniFrac distance rarefaction curves of each sample. Gut microbial composition at the phylum level (D) and class level (E) between sham ($n = 5$) and I/R groups ($n = 6$). Bubble chart distributing significantly different taxa at the phylum level (F) and class level (G) between sham ($n = 5$) and I/R groups ($n = 6$). (H) Relative abundance of Proteobacteria in the gut microbiome and proportion of subordinate Gammaproteobacteria in Proteobacteria phylum between sham ($n = 5$) and I/R groups ($n = 6$). (I) Gross morphology of the gastrointestinal tract from sham-operated mice and I/R injured mice 3 days after the operation. (J) Representative images of intestine Hematoxylin and Eosin (HE) staining of sham and I/R mice 3 days after the operation. (K) Intestine injury assessment of intestine HE staining in (J) presented as Chiu scores ($n = 5$). (L) Representative transmission electron microscope image of sections from the intestinal epithelium of sham and I/R mice. Scale bar = 2 μm . (M) Representative immunofluorescence images of claudin-1 in the intestine of sham and I/R mice 3 days after the operation. Scale bar = 50 μm . (N) Quantification of fluorescence intensity in (M) ($n = 5$). Values are mean \pm SD. Statistical significance was determined using Student's *t*-test or Mann-Whitney *U* test for the two group comparison. * $P < 0.05$, ** $P < 0.01$, *** $P < 0.001$.

staining using antibodies against bacterial LPS and RNA fluorescence *in situ* hybridization (FISH) with a universal probe against bacterial 16S rRNA to detect bacteria distribution in heart tissues (Figure 3M and N). Fluorescence staining showed that bacterial LPS and 16S rRNA shared a similar spatial distribution, localized along the ischaemic region of heart tissue. Taken together, these data provided solid evidence that myocardial I/R injury increased gut permeability and thus promoted the translocation and dissemination of gut microbiota and bacterial products to circulation and subsequently extra-intestinal organs.

3.4 Gut microbiota translocation acted as a primary modifier determining the severity of myocardial I/R injury through modulating inflammation

We next investigated whether gut bacterial translocation directly contributed to the severity of myocardial I/R injury. We first conducted the myocardial I/R model in germ-free (GF) mice and found that GF mice developed

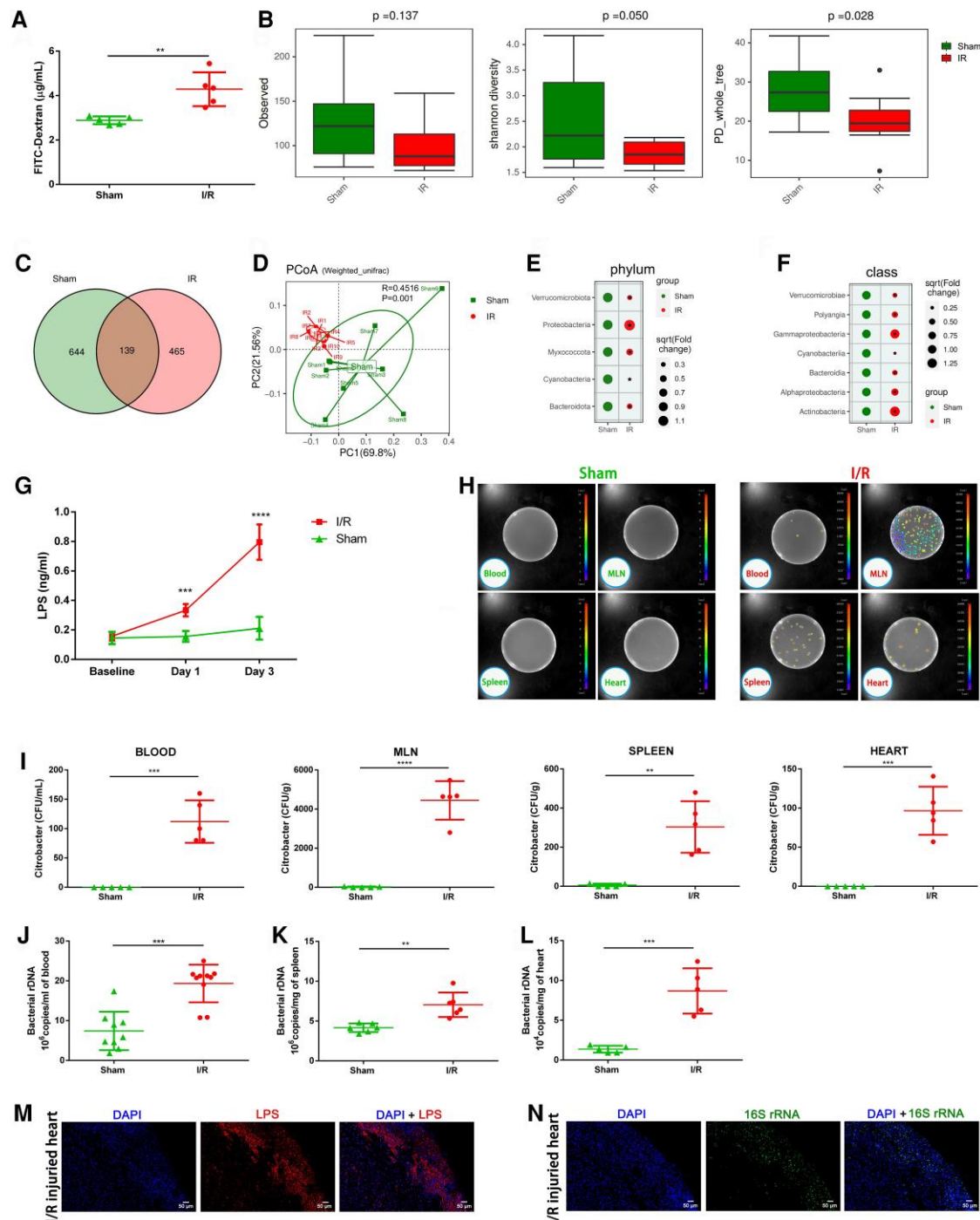


Figure 3 Increase in intestinal permeability upon myocardial I/R injury leads to gut microbiota translocation with an elevated level of LPS in circulation. (A) Intestinal permeability was measured by measuring plasma FITC-dextran level after oral administration of FITC-dextran on Day 3 after the operation ($n=5$). (B) Comparative analyses of blood microbial α -diversity estimated by Sobs, Shannon's diversity, and phylogenetic diversity (PD) between sham ($n=9$) and I/R groups ($n=10$). (C) The number of common and unique ASVs in the circulation of sham ($n=9$) and I/R mice ($n=10$) 3 days after the operation. (D) PcoA of blood microbial profiles based on weighted UniFrac analysis between sham ($n=9$) and I/R groups ($n=10$) distributing significantly different taxa of blood microbial profiles at the phylum level (E) and class level (F) between sham ($n=9$) and I/R groups ($n=10$). (G) Serum LPS concentration on Day 1 and Day 3 following the operation ($n=5$). (H) Bacterial colony forming units (CFUs) of sample homogenates obtained from various tissues of sham and I/R mice were visualized under an *in vivo* imaging system after oral gavage of Bioluminescent *C. rodentium* on Day 3 after the operation. (I) Quantification of CFU counts in (H) ($n=5$). (J) Quantification of blood bacterial load per millilitre based on 16S rDNA content collected from sham ($n=9$) and I/R ($n=10$) mice 3 days following the operation. (K) Quantification of bacterial load per milligram within spleen tissues 3 days following the operation ($n=6$). (L) Quantification of bacterial load per milligram within heart samples collected from sham and I/R mice 3 days after the operation ($n=5$). Consecutive slices from I/R injured hearts were stained with anti-LPS antibody (M) or with FISH probes against bacterial 16S rRNA (N). Scale bar = 50 μm . Values are mean \pm SD. Statistical significance was determined using Student's *t*-test or Mann–Whitney *U* test for the two group comparison. * $P < 0.05$, ** $P < 0.01$, *** $P < 0.001$, **** $P < 0.0001$.

a smaller extent of MVO following myocardial I/R induction compared with age-matched specific pathogen-free mice based on thioflavin-S staining, suggesting the potential role of commensal bacteria in the development of myocardial I/R injury (Figure 4A). Considering the influence of GM on innate immunity,¹⁷ we then administered a mixture of antibiotics (ABX) orally to only pre-deplete the gut microbiota before injury. Quantification of bacterial load in faeces collected from ABX and untreated mice was examined to verify the depletion efficiency (see Supplementary material online, Figure S4A). Three days following myocardial I/R induction, an echocardiogram examination revealed that cardiac function was better preserved in ABX mice relative to untreated mice (Figure 4B and Supplementary material online, Figure S4B). Evans Blue and 2, 3, 5-triphenyl-2H-tetrazolium chloride (TTC) staining and thioflavin-S staining demonstrated that infarct size and MVO size were remarkably smaller in the ABX group when compared with the untreated group (Figure 4C and D). Collectively, these findings suggested a direct causal link between gut bacterial translocation and severity of myocardial I/R injury, especially in the initial stage of I/R injury.

To elucidate potential mechanisms of cardioprotective effect exerted by gut microbiota depletion, we examined the levels of inflammation-related biomarkers in mouse serum and found that pre-depletion of gut microbiota dramatically decreased serum LPS concentrations, accompanied by reduced levels of IL-6, IL-1 β , and TNF- α following myocardial I/R injury (Figure 4E and F). Accordingly, a significant reduction of inflammatory cell infiltration within ischaemic heart was observed in GF and ABX mice, suggesting the attenuation of cardiac inflammation following microbiota depletion (see Supplementary material online, Figure S4C and D). We further performed flow cytometry analysis to assess the quantity and subpopulation of myeloid cells in the peripheral circulation of ABX and untreated mice. Flow cytometric analysis demonstrated a significant reduction of neutrophils, and monocytes, especially pro-inflammatory Ly6C^{high} monocytes, in the peripheral blood of ABX-treated myocardial I/R mice compared with that of the untreated myocardial I/R mice (Figure 4G and H). Furthermore, we observed the populations of neutrophils and monocytes in spleen and bone marrow (BM) using flow cytometry analysis (Figure 4I and J; Supplementary material online, Figure S5). As for the kinetic of neutrophils, BM output increased in response to myocardial I/R injury as expected. The quantity of neutrophils in the BM was higher in the ABX-I/R group than that of the untreated-I/R group, indicating that abrogation of gut bacterial translocation might compromise the mobilization of neutrophils from BM. On the other hand, more splenic monocytes, including both Ly6C^{high} and Ly6C^{low} monocytes, were preserved in the spleen of ABX-I/R mice relative to untreated-I/R mice, whereas no differences were detected in BM. The spleen acted as a monocyte reservoir in the early stage of myocardial I/R injury, whereas depletion of gut microbiota could restrain the recruitment of splenic monocytes. Taken together, these results implied that bacterial translocation products aggravated inflammation by promoting myeloid cell migration from BM or spleen reservoir and thus worsen myocardial I/R injury.

3.5 Glucagon-like peptide 2 administration restored gut microbiota disorder, strengthened the gut mucosa barrier, and prevented microbiota translocation following myocardial I/R injury

Based on our data, we hypothesized that the heart–gut–microbiome–immune axis might be a novel therapeutic target for ameliorating excessive inflammation in myocardial I/R injury. Numerous attempts have been made to restore healthy microbiota and strengthen gut barrier function, but the therapeutic effect is not ideal and the translational value is limited. The administration of broad-spectrum antibiotics to eliminate the intestinal microbiota could cause life-threatening antibiotic resistance and increase the risk of heart rupture.¹¹ Additionally, probiotic supplementation and faecal bacteria transplantation take a long time to exert their therapeutic effect, which limited their application in acute diseases.^{18,19}

Glucagon-like peptide 2 (GLP-2), a 33-amino acid peptide produced by intestinal endocrine L-cells, has been demonstrated to enhance gut barrier function and induce intestinal mucosa proliferation in a variety of intestinal pathological conditions.^{20,21} Circulating level of GLP-2 was recently found to be increased in patients with AML.²² Therefore, we determined to investigate whether GLP-2 could protect the gut barrier, restore intestinal microbiota dysbiosis, and thus alleviate gut microbial translocation under myocardial I/R injury. We first induced myocardial I/R injury in mice, 600 μ g/kg degradation-resistant GLP-2 analogue dissolved in saline was injected subcutaneously immediately after reperfusion and continuously delivered twice daily for 3 days. The dose of GLP-2 was determined according to our preliminary dose-ranging experiment (see Supplementary material online, Figure S6). As expected, GLP-2 significantly attenuated intestinal mucosa injury (Figure 5A–C) and enhanced the intestinal mechanical barrier (Figure 5D). The expression of tight-junction protein Occludin and Claudin-1 increased in GLP-2-treated mice when compared with saline-treated mice, indicating the positive effect of GLP-2 on tight-junction integrity (Figure 5E and F; Supplementary material online, Figure S7). Consistent with these changes, intestinal permeability decreased following GLP-2 treatment (Figure 5G). These findings revealed that GLP-2 could effectively rescue intestinal barrier dysfunction and gut permeability elevation induced by myocardial I/R injury.

We further investigated the effect of GLP-2 treatment on intestinal microbiota dysbiosis. 16S rRNA gene sequencing analysis of intestinal microbial communities showed a dramatic restoration of intestinal bacteria dysbiosis after GLP-2 administration, manifested as significant inhibition of the overgrowth of pro-inflammatory Proteobacteria phylum and its subordinate Gammaproteobacteria class (Figure 5H–J; see Supplementary material online, Figure S8A–G). Coinciding with the restoration of the intestinal microbiome, GLP-2 significantly normalized the disrupted blood microbial community almost to the sham group level and partially restored the microbiota diversity under myocardial I/R injury (Figure 5K–N; Supplementary material online, Figure S8H and I). 16S rDNA quantitation by real-time qPCR further confirmed that blood bacterial load was remarkably reduced in GLP-2-treated mice relative to vehicle (saline) control (Figure 5O). Meanwhile, LPS levels were significantly lower in the serum of GLP-2-treated mice when compared with the saline-treated group on Day 1 and Day 3 post-myocardial I/R induction (Figure 5P). In bioluminescent *C. rodentium* inoculation experiment, we disclosed that GLP-2 obviously attenuated bacterial translocation into circulation, MLNs, spleen, and heart after myocardial I/R injury (Figure 5Q and R). Taken together, the results described above declared that GLP-2 exerted a protective role in maintaining the integrity of the intestinal barrier and homeostasis of the intestinal microbiome, thus defending gut bacterial translocation after myocardial I/R injury.

3.6 GLP-2 attenuated myocardial I/R injury by alleviating inflammation induced by gut bacterial translocation

Next, we investigated whether GLP-2 treatment exerted a curative effect on myocardial I/R injury. GLP-2 treatment efficiently reversed the decrease of cardiac ejection fraction (EF%) and fractional shortening (FS%) in mice under myocardial I/R injury (Figure 6A). Reduced infarct size, attenuated MVO, and decreased cardiomyocyte apoptosis were detected in GLP-2-treated mice relative to vehicle control in the acute phase of myocardial I/R injury (Figure 6B–D). During the chronic repair phase, the benefits of GLP-2 still existed, leading to a restored survival rate, preserved left ventricular systolic and diastolic dimensions, attenuated fibrosis, and reduced cardiomyocyte hypertrophy (see Supplementary material online, Figure S9). These results demonstrated that GLP-2 not only exerted protective effects in the initial stage of myocardial I/R injury but also conferred sustained beneficial effects on cardiac repair.

To uncover the linkage between the benefits of GLP-2 and its prevention of bacterial translocation, we focused on inflammation-associated alterations after GLP-2 administration. Reduced inflammatory cell

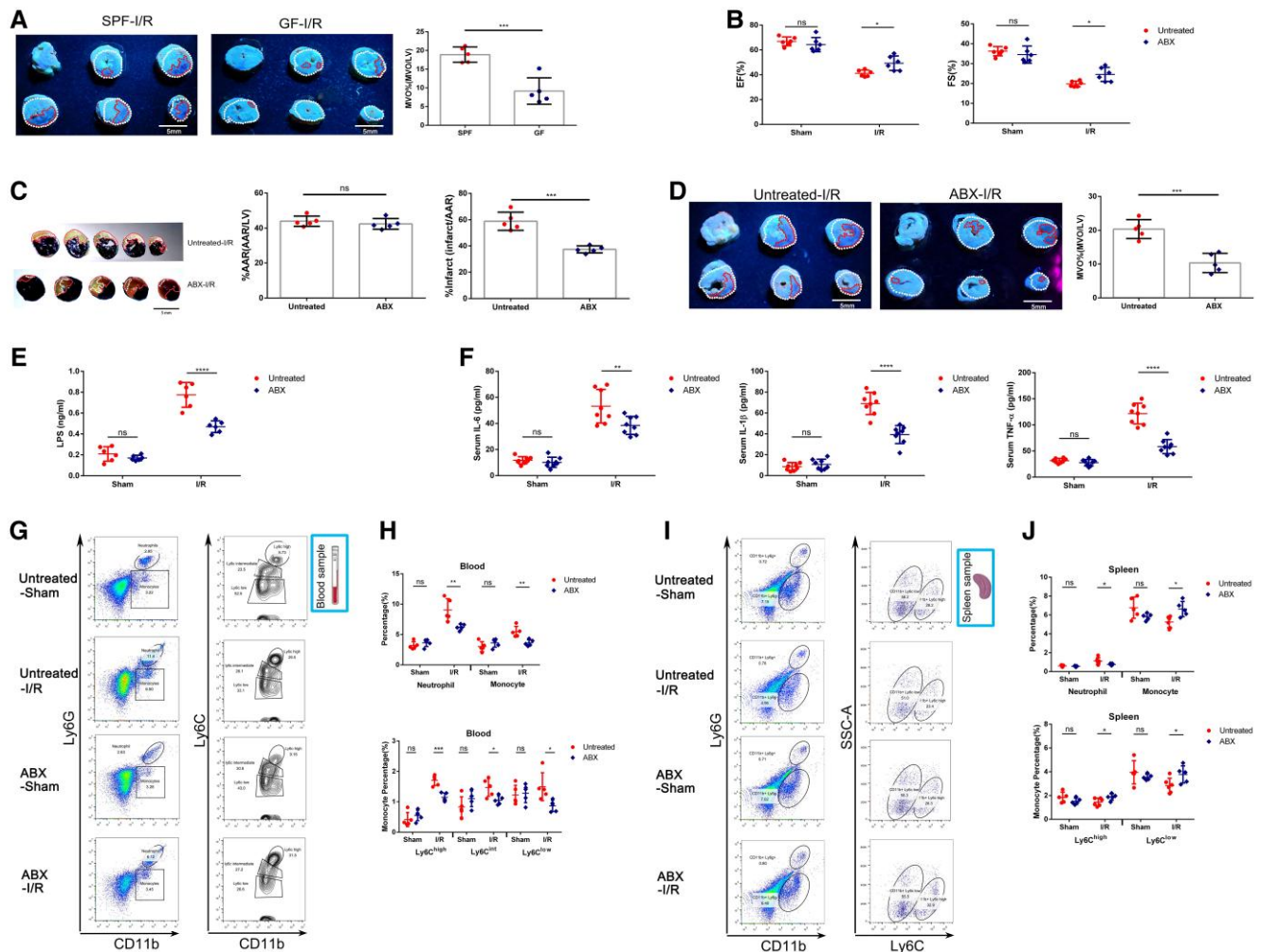


Figure 4 Pre-depletion of gut microbiota ameliorates myocardial I/R injury and systemic inflammation in mice. (A) Representative thioflavin-S stained images showing MVO regions indicated by the absence of thioflavin-S fluorescence and quantification of MVO percentage in hearts collected from GF and specific pathogen-free (SPF) mice 1 day following myocardial I/R injury ($n = 5$). Left ventricular area (LV; white dotted line) and MVO size (MVO; red dotted line). Scale bar = 5 mm. (B) ejection fraction (EF%) and fractional shortening (FS%) of a mixture of antibiotics (ABX) treated and untreated mice measured by echocardiography 3 days following myocardial I/R injury ($n = 6$). (C) Representative images of Evans Blue and TTC-stained hearts and quantification of the percentage Area at risk (AAR) and percentage infarct in ABX and untreated mice 3 days after myocardial I/R injury ($n = 5$). AAR (red line) and infarct size (IS; white dotted line). Scale bar = 5 mm. (D) Representative thioflavin-S stained images and quantification of MVO percentage in hearts isolated from ABX and untreated mice 1 day following myocardial I/R injury ($n = 5$). Left ventricular area (LV; white dotted line) and MVO size (MVO; red dotted line). Scale bar = 5 mm. (E) The serum level of LPS in ABX and untreated mice 3 days after myocardial I/R injury ($n = 6$). (F) Serum IL-6, IL-1 β , and TNF- α levels of ABX and untreated mice 3 days after the operation ($n = 8$). (G) Representative flow cytometry plots showing the gating strategy used to determine total neutrophils (CD11b⁺ Ly6G⁺), total monocytes (CD11b⁺ Ly6G⁻ Ly6C⁺), Ly6C^{high} monocytes (CD11b⁺ Ly6G⁻ Ly6C^{high}), Ly6C^{int} monocytes (CD11b⁺ Ly6G⁻ Ly6C^{intermediate}), and Ly6C^{low} monocytes (CD11b⁺ Ly6G⁻ Ly6C^{low}) in peripheral blood 3 days following the operation. (H) Quantification of total neutrophils, total monocytes, Ly6C^{high} monocytes, Ly6C^{int} monocytes, and Ly6C^{low} monocytes in the peripheral blood of ABX and untreated mice 3 days following myocardial I/R injury ($n = 5$). (I) The ratio of total neutrophils, total monocytes, Ly6C^{high} monocytes, and Ly6C^{low} monocytes was analysed by fluorescence-activated cell sorter in spleen of ABX and untreated mice at 3 days post-operation. (J) Pooled flow cytometry data from (I) ($n = 5-6$). Values are mean \pm SD. Statistical significance was determined using Student's *t*-test for the two group comparison or two-way ANOVA followed by Bonferroni's multiple comparisons test for comparison between different groups. * $P < 0.05$, ** $P < 0.01$, *** $P < 0.001$, **** $P < 0.0001$, ns = not significant.

infiltration was observed in GLP-2-treated mice (Figure 6E), as well as a significant decrease of IL-6, IL-1 β , and TNF- α levels in heart tissues and serum (Figure 6F and G). Meanwhile, the serum IL-10 concentration was significantly increased in GLP-2-treated mice relative to saline-treated animals (Figure 6G). Flow cytometry analysis indicated that the proportions of neutrophils and macrophages, especially inflammatory macrophages (iNOS⁺ CD206⁺), in ischaemic hearts were obviously decreased upon GLP-2

treatment (Figure 6H and I). Flow cytometric analysis of peripheral blood showed a significant reduction of neutrophils and monocytes, especially pro-inflammatory Ly6C^{high} monocytes in GLP-2-treated mice relative to saline-treated mice (see Supplementary material online, Figure S10A and B). Furthermore, an increased number of splenic monocytes, including both Ly6C^{high} and Ly6C^{low} monocytes, were preserved in the spleen of GLP-2-treated mice in comparison to saline-treated mice, underlying the

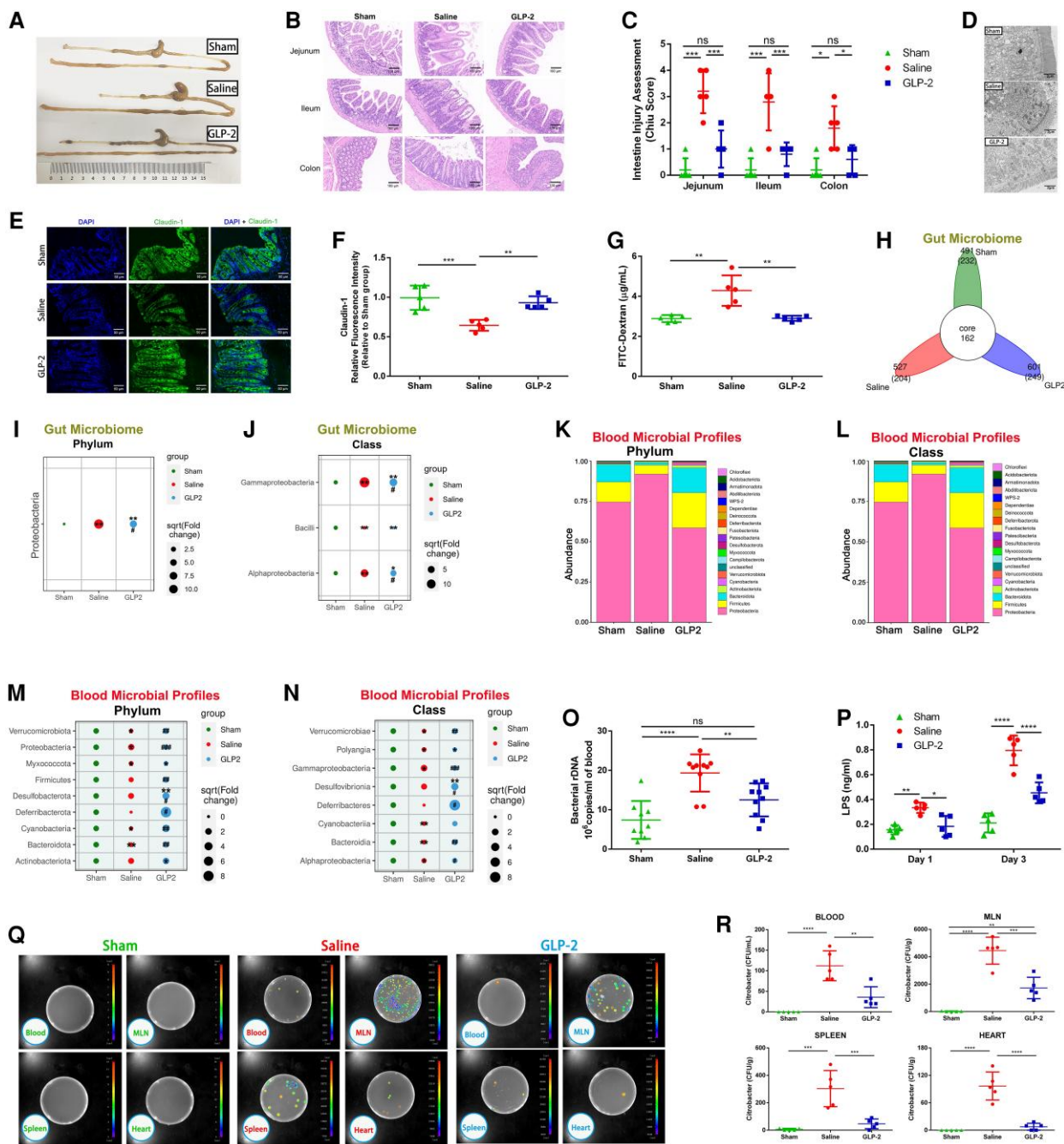


Figure 5 GLP-2 ameliorates gut microbiota disorder, suppresses gut barrier dysfunction, and prevents microbiota translocation following myocardial I/R injury. (A) Gross morphology of the gastrointestinal tract from mice 3 days following treatment with saline or GLP-2 3 days after the operation. (B) Representative images of intestine HE staining of mice sacrificed 3 days after myocardial I/R injury. (C) Intestine injury assessment of intestine HE staining in (B) presented as Chiu scores (n = 5). (D) Representative image of intestinal epithelium structure of sham-operated, saline-treated, or GLP-2-treated mice detected by transmission electron microscope. Scale bar = 2 μ m. (E) Representative immunofluorescence images of claudin-1 in the intestine of mice 3 days after the operation. Scale bar = 50 μ m. (F) Quantification of fluorescence intensity in (E) (n = 5). (G) Intestinal permeability was measured by detecting plasma FITC-dextran level after oral administration of FITC-dextran on Day 3 of myocardial I/R injury (n = 5). (H) The number of common and unique ASVs in colon contents of mice 3 days post-I/R (n = 5–6). Bubble chart distributing significantly different taxa of gut microbiome at the phylum level (I) and class level (J) among groups (n = 5–6). Blood microbial composition at the phylum level (K) and class level (L) among sham-operated (n = 9), saline-treated (n = 10), and GLP-2-treated (n = 10) groups. Bubble chart distributing significantly different taxa of blood microbial profiles at the phylum level (M) and class level (N) among groups. (O) Quantification of blood bacterial load per millilitre based on 16S rDNA content 3 days following the operation (n = 9–10). (P) Concentration of LPS in serum on Day 1 and Day 3 of myocardial I/R injury (n = 5). (Q) Bacterial CFUs of sample homogenates isolated from various tissues of sham-operated, saline-treated, and GLP-2-treated mice were visualized under an *in vivo* imaging system after oral gavage of Bioluminescent *C. rodentium* on Day 3 after the operation. (R) Quantification of CFU counts in (Q) (n = 5). Values are mean \pm SD. Statistical significance was determined using one-way ANOVA followed by Tukey's multiple comparisons test for multiple group comparisons. * P < 0.05, ** P < 0.01, *** P < 0.001, **** P < 0.0001, ns = not significant. # P < 0.05, ## P < 0.01, ### P < 0.001 compared with the I/R group.

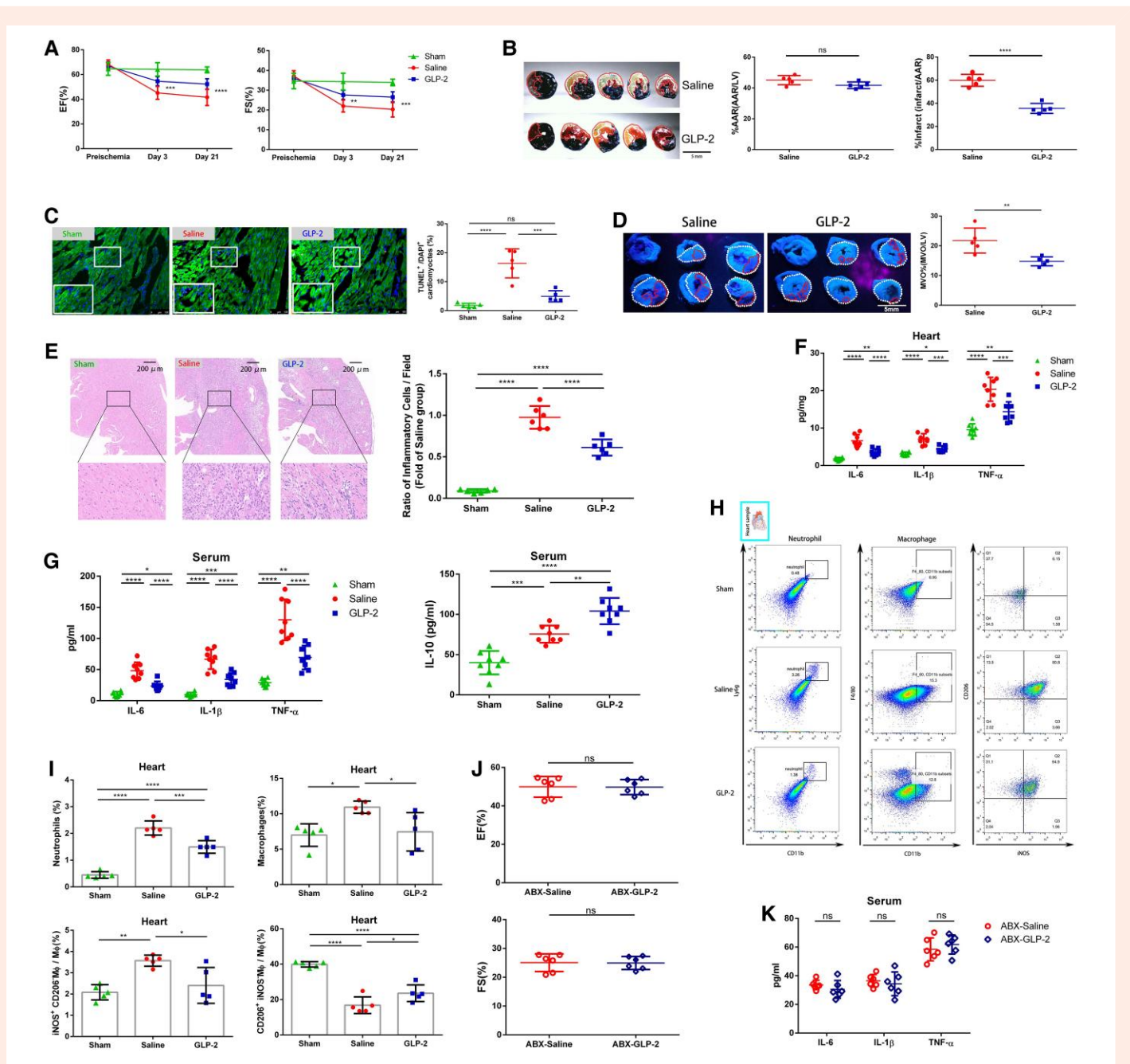


Figure 6 Inhibiting intestinal microbiota translocation by administering GLP-2 attenuates myocardial I/R injury and alleviates cardiac inflammation in mice. (A) Quantitative analysis of EF% and FS% of mice treated with saline or GLP-2 measured by echocardiography 3 days and 3 weeks following myocardial I/R injury ($n=9$). (B) Representative images of Evans Blue and TTC-stained hearts and quantification of the percentage AAR and percentage infarct in myocardial I/R injured mice 3 days following treatment with saline or GLP-2. AAR (red line) and infarct size (IS; white dotted line). Scale bar = 5 mm. (C) Representative images of TUNEL-stained heart tissues and quantification of the percentage of TUNEL⁺ cardiomyocytes within the infarct zones of saline- or GLP-2-treated mice 24 h post-I/R ($n=5$). Scale bar = 100 μ m. (D) Representative thioflavin-S stained images and quantification of MVO percentage in hearts isolated from saline- or GLP-2-treated mice 1 day following myocardial I/R injury ($n=5$). Left ventricular area (LV; white dotted line) and MVO size (MVO; red line). Scale bar = 5 mm. (E) Representative images of HE staining and quantification of inflammatory cell infiltration (%) within the ischaemic heart of saline- and GLP-2 treated mice 3 days following the operation ($n=6$). Scale bar = 200 μ m. (F) Cytokine expression of IL-6, IL-1 β , and TNF- α in the hearts of mice treated with saline or GLP-2 3 days post-I/R ($n=8$). (G) Serum IL-6, IL-1 β , TNF- α , and IL-10 levels of mice treated with saline or GLP-2 3 days after the operation ($n=8$). (H) Representative flow cytometry plots for cardiac tissue in sham-operated, saline-treated, or GLP-2-treated I/R injured mice 3 days post-operation. Live cells were gated with CD11b and Ly6G positive (CD11b⁺ Ly6G⁺) population to identify neutrophils, CD11b, and F4/80 positive (CD11b⁺ F4/80⁺) population to identify macrophages. Macrophages were then gated into iNOS⁺ CD206⁻ population and iNOS⁻ CD206⁺ population. (I) Pooled flow cytometry data in H ($n=5$). (J) EF% and FS% of ABX-saline and ABX-GLP-2 mice measured by echocardiography 3 days following myocardial I/R injury ($n=6$). (K) Serum IL-6, IL-1 β , and TNF- α levels of ABX-saline and ABX-GLP-2 mice 3 days after the operation ($n=6$). Values are mean \pm SD. Statistical significance was determined using Student's *t*-test for the two group comparison (Figure 6B, D, J, and K), one-way ANOVA followed by Tukey's multiple comparisons test for multiple group comparisons (Figure 6C, E–G, and I), and two-way ANOVA followed by Bonferroni's multiple comparison test for comparison between different groups over time (Figure 6A). * $P < 0.05$, ** $P < 0.01$, *** $P < 0.001$, **** $P < 0.0001$, ns, not significant.

inhibitory effect of GLP-2 on splenic monocyte migration (see [Supplementary material online, Figure S10C and D](#)). Intriguingly, we observed a trend of increase in neutrophils in the spleen of saline-treated mice, which was rescued upon GLP-2 administration. These might be due to the prevention of gut bacterial translocation to spleen by GLP-2, which alleviates local inflammation in spleen. Collectively, these data demonstrated that GLP-2 could significantly reduce inflammatory cell recruitment and restrain the migration of monocytes from the spleen reservoir.

To further clarify whether the curative and immunomodulatory effect of GLP-2 was mediated by its impact on gut microbiota, we treated mice with ABX to pre-deplete gut microbiota before myocardial I/R induction and then treated the mice with saline or GLP-2 immediately after reperfusion. As anticipated, GLP-2 lost the therapeutic effect of improving cardiac function and attenuating inflammation under gut microbiota pre-depletion circumstances ([Figure 6J and 6K](#)), suggesting that the potential effects of GLP-2 were ascribed to its impact on gut microbiota. We further built the macrophage depletion model²³ and found that depletion of macrophages impaired the curative effects of GLP-2 (see [Supplementary material online, Figure S11](#)), suggesting that macrophages might be involved in the cardioprotective effect of GLP-2.

4. Discussion

In this study, we unravelled a novel, bidirectional communication along the heart–gut–microbiome–immune axis during myocardial I/R injury. We demonstrated that myocardial I/R injury itself induced intestinal microbial alteration and gut barrier disruption thus leading to bacterial translocation and that these changes in turn aggravated I/R injury by augmenting inflammation. New therapeutic intervention by GLP-2 targeting gut bacteria dysbiosis and translocation might be a potential strategy to alleviate excessive inflammation activation under myocardial I/R injury ([Graphical abstract](#)).

In our study, the gut microbiota dysbiosis, rapidly induced by I/R injury, was characterized as an overgrowth of Proteobacteria and its family Enterobacteriaceae. Recently, emerging evidence indicated that the blooming of Proteobacteria in gut could disrupt the intestinal microbiota homeostasis, trigger mucosal inflammation activation, and subsequently, contribute to the destruction of the intestinal barrier.²⁴ In line with changes in gut microbiota, we observed remarkable intestinal mucosa injury and tight-junction disruption in myocardial I/R injured mice. However, the detailed mechanism of gut barrier dysfunction under myocardial I/R injury was not fully elucidated. In addition to gut microbiota dysbiosis, intestinal hypo-perfusion,^{12,25} reduced gastrointestinal motility, and severe gastrointestinal paralysis²⁶ might contribute to the impairment of gut barrier integrity. Fully clarifying the decisive factors of gut microbiota dysbiosis and intestinal barrier dysfunction under myocardial I/R injury requires further study.

The inflammatory cascade induced by myocardial I/R was traditionally considered as aseptic inflammation. Although recent significant studies shed light on the potential association between gut bacteria and severity of MI,²⁷ convincing evidence of bacteria translocation was still lacking. To the best of our knowledge, the present study first presented direct evidence for the occurrence of gut bacteria translocation under myocardial I/R injury. The bioluminescent *C. rodentium* inoculation experiment and 16S rDNA qPCR provided solid evidences to demonstrate that intestinal-derived bacteria could translocate and disseminate into circulation, MLN, and even the spleen and heart after induction of myocardial I/R injury.

Considering the potential role of gut bacteria translocation in the exacerbation of both local and systemic inflammation, we investigated whether gut leakage induced by I/R injury might aggravate myocardial I/R injury in turn. Studies in GF mice show a global defect in myeloid cell populations at primary immune sites,¹⁷ indicating the lack of a mature immune system in GF mice. Therefore, we determined the effect of gut microbiota translocation on myocardial I/R injury severity using both GF mice and orally gavage a mixture of antibiotics to pre-deplete the gut microbiota before injury. We found that pre-depletion of gut microbiota led to remarkable protective effects on myocardial I/R injury. Our observations

in the clinical cohort of STEMI patients further supported that higher levels of LPS and blood bacterial load were associated with larger infarct size, extensive MVO, and compromised cardiac function in patients with STEMI. However, the present study fails to prove a clear causality of gut bacteria translocation in STEMI patients, which cannot be assessed in the performed observational cross-sectional cohort study design with limited duration. Thus, the results might be considered as hypothesis-generating, and the ongoing follow-up study may yield more conclusive data. Taken together, our results suggested that gut bacteria translocation was not only the consequence of myocardial I/R injury but also might be one of the primary modifiers in determining its outcome.

Intestinal microbiota have been reported to influence the composition, migration, and function of various immune cell subpopulations and thus affecting host immune homeostasis.²⁸ Danilo et al.²⁹ reported that oral administration of Bifidobacterium to reverse gut microbiota dysbiosis significantly mitigated the pathological impact of MI through enhancing global acetylation of Treg cells. Our data demonstrated that the accumulation of translocated bacteria promoted neutrophil and monocyte infiltration via promoting the migration of neutrophils from BM and recruitment of monocytes from the spleen reservoir after myocardial I/R injury. The detailed mechanism between gut bacteria translocation and myeloid cell mobilization was still not fully elucidated. LPS has been implicated as the major harmful component of bacteria and largely decides the pro-inflammatory effect of gram-negative bacteria.^{8,30} Under the basal condition, LPS from the gut microbiota was observed to be accumulated in BM and initiated Nod1-dependent myeloid cell activation³¹. Meanwhile, LPS was reported to enhance monocytes and neutrophils activation via Toll-like receptor 4 (TLR4)-dependent and TLR4-independent signalling pathways in multiple pathological conditions.^{13,32} Therefore, LPS might serve as a non-negligible factor accounting for the aggravation of inflammation in myocardial I/R injury. Recent studies have also suggested that intestinal microbiota dysbiosis could activate intestinal T helper type 17 (Th17) cells and promote the secretion of IL-17.³³ It is reported that IL-17 mediates progenitor neutrophil expansion and mature neutrophils in the peripheral blood by inducing expression of granulocyte colony-stimulating factor and chemokines such as CXCL-1, CXCL-2, and CXCL-5.³⁴ Park et al.³⁵ showed that acute kidney injury rapidly resulted in the intestinal generation of IL-17A, which led to increased production of IL-6 and TNF- α , thus eventually initiated systemic inflammation. These findings provided another possibility that IL-17 secreted by intestinal Th17 cells might be involved in the modulation of inflammation intensity under myocardial I/R injury.

The novel findings in the current study indicated that the prevention of gut microbiota dysbiosis and translocation might be a potential target for the treatment of myocardial I/R injury. Glucagon-like peptide 1 (GLP-1) and GLP-2 are gut-derived hormones that are co-secreted from intestinal L-cells. While GLP-1 has been extensively studied in cardiovascular diseases,³⁶ the effect and underlying mechanism of GLP-2 in cardiovascular diseases remains elusive.³⁷ GLP-2 has been demonstrated to enhance intestinal epithelial proliferation and is clinically used for the treatment of short bowel syndrome.³⁸ Significant studies in recent years disclosed that the protective effect of GLP-2 was not only restrained to intestine but also existed in liver and brain injury.^{39,40} The cardiovascular systemic response to GLP-2 has been reported in both animal and human studies,⁴¹ while the underlying mechanism is undetermined. In our study, we first demonstrated that GLP-2 could restore gut microbiota dysbiosis and prevent gut bacteria translocation under myocardial I/R injury, thereby exerting a cardioprotective effect. The curative effect of GLP-2 has a strong relation with its attenuation of cardiac and systemic inflammation induced by translocated bacteria. Despite our study pinpointing the involvement of macrophages in the cardioprotective effect of GLP-2, our results do not exclude the possible involvement of other signalling pathways in the immunomodulatory effect of GLP-2. In addition, whether GLP-2 acts through coupling with unidentified receptors in macrophages directly or indirectly regulate macrophages by preventing bacteria translocation remains unclear and thus requires further study.

In summary, our study demonstrates a novel concept that gut microbiota dysbiosis and translocation is a consequence of myocardial I/R and

serves as a critical effector in promoting post-I/R inflammation overactivation, with considerable impact on the exacerbation of I/R injury. Microbiota depletion prior to injury supports this hypothesis and provides important insight into the influence of translocated bacteria on local and systemic inflammation. Finally, our study suggests that GLP-2 treatment targeting the bidirectional interaction between heart and intestine may represent a promising tool in ameliorating myocardial I/R injury.

Supplementary material

Supplementary material is available at *Cardiovascular Research* online.

Authors' contributions

J.Z., Q.Z., W.C., and J.X. designed the experiment and drafted the manuscript. Q.D., Z.W., M.G., and F.C. performed human samples data collection. J.Z., Q.Z., W.C., S.Q., J.H., J.W., and H.C. performed the animal experiments. X.B. and D.M. performed the statistical analyses of clinical data and interpreted the results. X.S., B.X., and J.X. supervised and provided comments for the manuscript.

Acknowledgements

The authors thank Professor Qingbo Xu for scientific advice and Professor Yun Zhang for technical assistance.

Conflict of interest: None declared.

Funding

This work was supported by the Natural Science Foundation of China (grant numbers 82000264, 82070366, 81870358, 92068116, and 82100533); the Jiangsu Provincial Key Research and Development Program (grant number BE2019602); Natural Science Foundation of Jiangsu Province (grant number BK20200139); the Natural Science Foundation of Jiangsu Province for Distinguished Young Scholars (grant number BK20211501); the Fundamental Research Funds for Central Universities (grant number 14380501); Jiangsu 'Mass Innovation and Entrepreneurship' Talent Program to Jinxuan Zhao.

Data availability

The data underlying this article are available in the article and in its online supplementary material.

References

- Heusch G. Myocardial ischaemia–reperfusion injury and cardioprotection in perspective. *Nat Rev Cardiol* 2020;**17**:773–789.
- Bekkers SCAM, Yazdani SK, Virmani R, Waltenberger J. Microvascular obstruction: underlying pathophysiology and clinical diagnosis. *J Am Coll Cardiol* 2010;**55**:1649–1660.
- Heusch G. Coronary microvascular obstruction: the new frontier in cardioprotection. *Basic Res Cardiol* 2019;**114**:45.
- Gomes AC, Hoffmann C, Mota JF. The human gut microbiota: metabolism and perspective in obesity. *Gut Microbes* 2018;**9**:308–325.
- Matson V, Chervin CS, Gajewski TF. Cancer and the microbiome–influence of the commensal microbiota on cancer, immune responses, and immunotherapy. *Gastroenterology* 2021;**160**:600–613.
- Gurung M, Li Z, You H, Rodrigues R, Jump DB, Morgun A, Shulzhenko N. Role of gut microbiota in type 2 diabetes pathophysiology. *EBioMedicine* 2020;**51**:102590.
- Katsimichas T, Antonopoulos AS, Katsimichas A, Ohtani T, Sakata Y, Tousoulis D. The intestinal microbiota and cardiovascular disease. *Cardiovasc Res* 2019;**115**:1471–1486.
- Zhang Y, Zhang S, Li B, Luo Y, Gong Y, Jin X, Zhang J, Zhou Y, Zhuo X, Wang Z, Zhao X, Han X, Gao Y, Yu H, Liang D, Zhao S, Sun D, Wang D, Xu W, Qu G, Bo W, Li D, Wu Y, Li Y. Gut microbiota dysbiosis promotes age-related atrial fibrillation by lipopolysaccharide and glucose-induced activation of NLRP3-inflammasome. *Cardiovasc Res* 2022;**118**:785–797.
- Lam V, Su J, Koprowski S, Hsu A, Tweddell JS, Rafiee P, Gross GJ, Salzman NH, Baker JE. Intestinal microbiota determine severity of myocardial infarction in rats. *FASEB J* 2012;**26**:1727–1735.
- Lam V, Su J, Hsu A, Gross GJ, Salzman NH, Baker JE. Intestinal microbial metabolites are linked to severity of myocardial infarction in rats. *PLoS One* 2016;**11**:e0160840.
- Tang TWH, Chen HC, Chen CY, Yen CYT, Lin CJ, Prajnamitra RP, Chen LL, Ruan SC, Lin JH, Lin PJ, Lu HH, Kuo CW, Chang CM, Hall AD, Vivas EI, Shui JW, Chen P, Hacker TA, Rey FE, Kamp TJ, Hsieh PCH. Loss of gut microbiota alters immune system composition and cripples postinfarction cardiac repair. *Circulation* 2019;**139**:647–659.
- Zhou X, Li J, Guo J, Geng B, Ji W, Zhao Q, Li J, Liu X, Liu J, Guo Z, Cai W, Ma Y, Ren D, Miao J, Chen S, Zhang Z, Chen J, Zhong J, Liu W, Zou M, Li Y, Cai J. Gut-dependent microbial translocation induces inflammation and cardiovascular events after ST-elevation myocardial infarction. *Microbiome* 2018;**6**:66.
- Carnevale R, Sciarretta S, Valenti V, di Nonno F, Calvieri C, Nocella C, Frati G, Forte M, d'Amati G, Pignataro MG, Severino A, Cangemi R, Arrivi A, Dominici M, Mangieri E, Gaudio C, Tanzilli G, Violi F. Low-grade endotoxaemia enhances artery thrombus growth via Toll-like receptor 4: implication for myocardial infarction. *Eur Heart J* 2020;**41**:3156–3165.
- Amar J, Lelouvier B, Servant F, Lluch J, Burcelin R, Bongard V, Elbaz M. Blood microbiota modification after myocardial infarction depends upon low-density lipoprotein cholesterol levels. *J Am Heart Assoc* 2019;**8**:e011797.
- Mouries J, Brescia P, Silvestri A, Spadoni I, Sorribas M, Wiest R, Mileti E, Galbiati M, Invernizzi P, Adorini L, Penna G, Rescigno M. Microbiota-driven gut vascular barrier disruption is a prerequisite for non-alcoholic steatohepatitis development. *J Hepatol* 2019;**71**:1216–1228.
- Zhang J, Yu WQ, Wei T, Zhang C, Wren L, Chen Q, Chen W, Qiu JY, Zhang Y, Liang TB. Effects of short-peptide-based enteral nutrition on the intestinal microcirculation and mucosal barrier in mice with severe acute pancreatitis. *Mol Nutr Food Res* 2020;**64**:e1901191.
- Khosravi A, Yáñez A, Price JG, Chow A, Merad M, Goodridge HS, Mazmanian SK. Gut microbiota promote hematopoiesis to control bacterial infection. *Cell Host Microbe* 2014;**15**:374–381.
- Gan XT, Ettinger G, Huang CX, Burton JP, Haist JV, Rajapurohitam V, Sidaway JE, Martin G, Gloor GB, Swann JR, Reid G, Karmazyn M. Probiotic administration attenuates myocardial hypertrophy and heart failure after myocardial infarction in the rat. *Circ Heart Fail* 2014;**7**:491–499.
- Drekonja D, Reich J, Gezahegn S, Greer N, Shaikat A, MacDonald R, Rutks I, Wilt TJ. Fecal microbiota transplantation for *Clostridium difficile* infection: a systematic review. *Ann Intern Med* 2015;**162**:630–638.
- Drucker DJ, Habener JF, Holst JJ. Discovery, characterization, and clinical development of the glucagon-like peptides. *J Clin Invest* 2017;**127**:4217–4227.
- Cheng W, Wang K, Zhao Z, Mao Q, Wang G, Li Q, Fu Z, Jiang Z, Wang J, Li J. Exosomes-mediated transfer of miR-125a/b in cell-to-cell communication: a novel mechanism of genetic exchange in the intestinal microenvironment. *Theranostics* 2020;**10**:7561–7580.
- Kahles F, Mertens RW, Rueckbeil MV, Arrivas MC, Moellmann J, Leberer C, Biener M, Giannitis E, Katus HA, Marx N, Lehrke M. The gut hormone GLP-2 predicts cardiovascular risk in patients with acute myocardial infarction. *Eur Heart J* 2020;**41**(Suppl. 2):1592.
- Zhao J, Li X, Hu J, Chen F, Qiao S, Sun X, Gao L, Xie J, Xu B. Mesenchymal stromal cell-derived exosomes attenuate myocardial ischaemia–reperfusion injury through miR-182-regulated macrophage polarization. *Cardiovasc Res* 2019;**115**:1205–1216.
- Shin NR, Whon TW, Bae JW. Proteobacteria: microbial signature of dysbiosis in gut microbiota. *Trends Biotechnol* 2015;**33**:496–503.
- Sandek A, Swidsinski A, Schroedel W, Watson A, Valentova M, Herrmann R, Scherbakov N, Cramer L, Rauchhaus M, Grosse-Herrenthey A, Krueger M, von Haehling S, Doehner W, Anker SD, Bauditz J. Intestinal blood flow in patients with chronic heart failure: a link with bacterial growth, gastrointestinal symptoms, and cachexia. *J Am Coll Cardiol* 2014;**64**:1092–1102.
- Singh V, Roth S, Llovera G, Sadler R, Garzetti D, Stecher B, Dichgans M, Liesz A. Microbiota dysbiosis controls the neuroinflammatory response after stroke. *J Neurosci* 2016;**36**:7428–7440.
- Hofmann R, Bäck M. Gastro-cardiology: a novel perspective for the gastrocardiac syndrome. *Front Cardiovasc Med* 2021;**8**:764478.
- Rooks MG, Garrett WS. Gut microbiota, metabolites and host immunity. *Nat Rev Immunol* 2016;**16**:341–352.
- Danilo CA, Constantopoulos E, McKee LA, Chen H, Regan JA, Lipovka Y, Lahtinen S, Stenman LK, Nguyen TV, Doyle KP, Slepian MJ, Khalpey ZI, Konhals JP. Bifidobacterium animalis subsp. lactis 420 mitigates the pathological impact of myocardial infarction in the mouse. *Benef Microbes* 2017;**8**:257–269.
- Xu K, Gao X, Xia G, Chen M, Zeng N, Wang S, You C, Tian X, Di H, Tang W, Li P, Wang H, Zeng X, Tan C, Meng F, Li H, He Y, Zhou H. Rapid gut dysbiosis induced by stroke exacerbates brain inflammation in turn. *Gut* 2021;**70**:1486–1494.
- Clarke TB, Davis KM, Lysenko ES, Zhou AY, Yu Y, Weiser JN. Recognition of peptidoglycan from the microbiota by Nod1 enhances systemic innate immunity. *Nat Med* 2010;**16**:228–231.
- Hagar JA, Powell DA, Aachoui Y, Ernst RK, Miao EA. Cytoplasmic LPS activates caspase-11: implications in TLR4-independent endotoxemic shock. *Science* 2013;**341**:1250–1253.
- Yang J, Kim CJ, Go YS, Lee HY, Kim MG, Oh SW, Cho WY, Im SH, Jo SK. Intestinal microbiota control acute kidney injury severity by immune modulation. *Kidney Int* 2020;**98**:932–946.

34. Pérez MM, Martins LMS, Dias MS, Pereira CA, Leite JA, Gonçalves ECS, de Almeida PZ, de Freitas EN, Tostes RC, Ramos SG, de Zoete MR, Ryffel B, Silva JS, Carlos D. Interleukin-17/interleukin-17 receptor axis elicits intestinal neutrophil migration, restrains gut dysbiosis and lipopolysaccharide translocation in high-fat diet-induced metabolic syndrome model. *Immunology* 2019;**156**:339–355.
35. Park SW, Chen SW, Kim M, Brown KM, Kolls JK, D'Agati VD, Lee HT. Cytokines induce small intestine and liver injury after renal ischemia or nephrectomy. *Lab Invest* 2011;**91**:63–84.
36. Heuvelman VD, Van Raalte DH, Smits MM. Cardiovascular effects of glucagon-like peptide 1 receptor agonists: from mechanistic studies in humans to clinical outcomes. *Cardiovasc Res* 2020;**116**:916–930.
37. Penna C, Pasqua T, Perrelli MG, Pagliaro P, Cerra MC, Angelone T. Postconditioning with glucagon like peptide-2 reduces ischemia/reperfusion injury in isolated rat hearts: role of survival kinases and mitochondrial KATP channels. *Basic Res Cardiol* 2012;**107**:272.
38. Hu X, Cheng W, Fan S, Huang Y, Chen X, Jiang Z, Wang J. Therapeutic potential of an intestinotrophic hormone, glucagon-like peptide 2, for treatment of type 2 short bowel syndrome rats with intestinal bacterial and fungal dysbiosis. *BMC Infect Dis* 2021;**21**:583.
39. Nuzzo D, Baldassano S, Amato A, Picone P, Galizzi G, Caldara GF, Di Carlo M, Mulè F. Glucagon-like peptide-2 reduces the obesity-associated inflammation in the brain. *Neurobiol Dis* 2019;**121**:296–304.
40. Topaloğlu N, Küçük A, Yıldırım Ş, Tekin M, Erdem H, Deniz M. Glucagon-like peptide-2 exhibits protective effect on hepatic ischemia-reperfusion injury in rats. *Front Med* 2015;**9**:368–373.
41. Bremholm L, Hornum M, Andersen UB, Hartmann B, Holst JJ, Jeppesen PB. The effect of Glucagon-Like Peptide-2 on mesenteric blood flow and cardiac parameters in end-jejunosotomy short bowel patients. *Regul Pept* 2011;**168**:32–38.

Translational perspective

This study demonstrates a unique bidirectional communication along the heart–gut–microbiome–immune axis in myocardial I/R injury. Myocardial I/R injury induced gut microbiota dysbiosis and gut barrier disruption thus leading to bacterial translocation and these changes in turn aggravated I/R injury by augmenting inflammation. Furthermore, our study sheds new light on the application of GLP-2 as a promising therapy targeting gut bacteria translocation in myocardial I/R injury. These findings highlight the gut microbiota targeting therapy as a potential therapeutic strategy to attenuate myocardial I/R injury and are of great translational value.